

Phase Transformation of AlAs to NiAs Structure at High Pressure

Raymond G. Greene, Huan Luo, Ting Li, and Arthur L. Ruoff

Department of Materials Science and Engineering, Cornell University, Ithaca, New York 14853

(Received 12 January 1994)

The crystal structure of AlAs has been studied in a diamond anvil cell using energy-dispersive x-ray diffraction to 46 GPa. AlAs undergoes a first order phase transformation from zinc blende to NiAs structure. This is the first experimental observation of a III-V compound transforming to the NiAs structure. The decrease in volume on transformation is $17 \pm 1\%$ at 7 GPa. The transformation is reversible but has large hysteresis. The equilibrium transformation pressure is 7 ± 5 GPa. Equations of state were obtained for both phases. The bulk modulus at zero pressure, B_0 , of zinc blende AlAs was measured to be 74 ± 4 GPa. These results are in good agreement with theoretical calculations.

PACS numbers: 64.70.Kb, 61.10.-i, 62.50.+p, 64.30.+t

The III-V compound semiconductor AlAs is of both technological and scientific interest. AlAs is the end point in the GaAs-AlAs ternary system which is the most important heterojunction system in III-V technology. The almost perfect lattice match between AlAs and GaAs is the foundation of various heteroepitaxial techniques used to fabricate heterostructures and superlattices between $\text{Al}_x\text{Ga}_{1-x}\text{As}$ and GaAs. The behavior of electrons in such systems is explained in terms of quantum wells, and the resulting structures have unique electrical and optical characteristics. Applications are generally limited to the $x < 0.3$ region of composition where $\text{Al}_x\text{Ga}_{1-x}\text{As}$ has a direct band gap. Examples of devices based on such structures include: heterojunction bipolar transistors (HBT), Bragg reflector superlattices, solid-state lasers, and high-electron-mobility transistors (HEMT) [1].

Like many other semiconductors that have tetrahedral structures at 1 atm, AlAs is expected to undergo a first order phase transition from the zinc blende structure to a sixfold coordinated structure at high pressure with $\sim 17\%$ volume change. Froyen and Cohen, and in a separate calculation Martin, on the basis of *ab initio* pseudopotential calculations, suggested the high pressure structure could be either rock salt or NiAs [2,3]. Weinstein *et al.* observed a phase transformation by microscopic examination at 12.3 GPa on loading but the structure was unknown [4].

Understanding the sequence of high pressure structures for the $A^N B^{N-8}$ compounds where A is aluminum is also of interest as a part of the larger goal of understanding the sequence for the $A^N B^{N-8}$ compounds in general. It is known that AlN transforms from wurtzite to rock salt [5], and that AlSb transforms from zinc blende to β -tin [6], in both cases with a decrease in volume of about 17%. This volume change is characteristic of transitions from fourfold to sixfold coordination in the III-V compounds, Ge, and Si. Previously, few measurements have been made on bulk AlAs because it is quite hygroscopic. This work, in determining the high pressure structure of AlAs is significant in that now only the high pressure structure of AlP remains unknown in this homologous

series.

This paper describes the high pressure x-ray diffraction experiment we have performed on AlAs to determine the new high pressure structure. In what follows we explain the experimental details and describe the results; these results are then discussed in the context of other calculations and experimental work.

The crystal structure of AlAs at 1 atm and room temperature is zinc blende ($B3$) with $a_0 = 5.660 \text{ \AA}$ [7]. The sample consisted of finely ground AlAs powder of 99.9% purity. The pressure vessel consisted of a diamond anvil cell (DAC) of the controlled displacement type. Diamond anvils with $300 \mu\text{m}$ flats were used. The sample chamber was a $100 \mu\text{m}$ diam hole in a spring steel gasket preindented to $50 \mu\text{m}$. A small amount of gold powder was also placed in the sample chamber to be used as a pressure marker. Three separate experiments were performed. In two of the experiments the AlAs sample had no exposure to moisture; the opening of the argon sealed package of AlAs from the vendor, sample grinding, DAC sample loading, and closing of the DAC, were all performed in a glove box with dry argon environment. The glove-box loaded sample experiments had lower diffuse backgrounds in their diffraction spectra than the non-glove-box prepared AlAs.

Energy dispersive x-ray diffraction (EDXD) experiments were performed at the Cornell High Energy Synchrotron Source (CHESS) to measure the equation of state (EOS) of the AlAs sample. Further details of the experimental techniques and apparatus are given in Refs. [8] and [9]. The diffraction geometry was calibrated with a gold foil. Diffraction angles 2θ of 14.095° and 16.967° were used. The typical collection time for a spectrum was approximately 20 min. The pressure for each spectrum was determined from the isothermal EOS of gold by Jamieson, Fritz, and Manghnani [10] from the x-ray measured gold cell volume. The sample cell volume was also obtained from each x-ray spectrum. Thus each spectrum represents a point of the sample EOS. The pressure was then increased (decreased) by decreasing (increasing) the anvil separation and the measured EOS was generated.

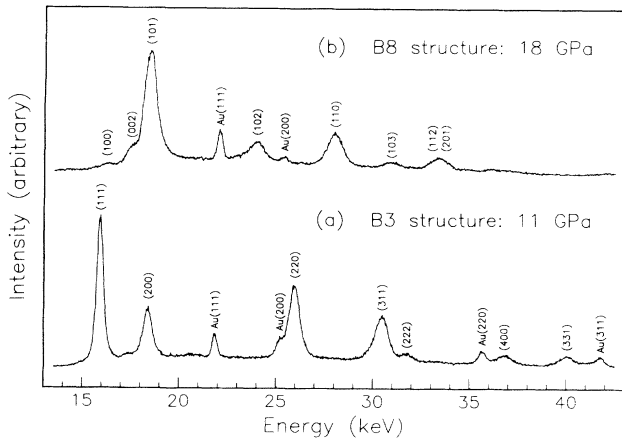


FIG. 1. EDXD diffraction spectra of AlAs. Au is gold; all other labeled peaks are the sample. (a) Original zinc blende structure near 11 GPa. (b) The new high pressure NiAs structure at 18 GPa.

On uploading from 0 to $P < 12$ GPa all spectra indexed very well to the initial $B3$ phase. Figure 1(a) shows a typical EDXD spectrum of AlAs near 11 GPa indexed to the $B3$ structure, before the phase transformation begins. Table I shows the observed and calculated d spacings, and integrated intensities. The agreement of the d spacings is excellent, but the integrated intensities have only fair agreement. This is typical for DAC EDXD experiments in which the sample is also the pressure medium so that deformation under loading often exacerbates texturing and preferred orientation to give a less than ideal powder diffraction pattern. This should be compared to a case where a quasihydrostatic pressure was obtained by use of a pressure medium (see Table I of Ref. [8]).

The EOS of the $B3$ phase is plotted in Fig. 2. These data were fitted to the first order Birch EOS:

$$P = \frac{3}{2} B_0 (x^{7/3} - x^{5/3}) [1 + \frac{3}{4} (B'_0 - 4)(x^{2/3} - 1)], \quad (1)$$

where $x = V_0/V$, B_0 is the isothermal bulk modulus at zero pressure, and B'_0 is the pressure derivative of the isothermal bulk modulus evaluated at zero pressure [11]. The resulting values of the two parameters are $B_0 = 74 \pm 4$ GPa, and $B'_0 = 5.0 \pm 1$. Our data fits equally well to the Murnaghan EOS [12], i.e., the values of B_0 , and B'_0 , change by 0.7%, and 6%, respectively.

For spectra with pressures ≥ 12 GPa there was a dramatic change in the pattern of the sample diffraction lines, indicating a phase transformation. The new pattern was stable above 14 GPa. Thus the following sequence of phases on uploading: $B3$ for $0 \leq P < 12$ GPa, mixed for $12 \leq P \leq 14$, and new phase for $P > 14$ GPa.

In order to determine the structure of the new phase the following two assumptions are made: (1) $\sim 17\%$ volume change (decrease) from the original to the new phase, and (2) the new phase has sixfold coordination vs the fourfold coordination of the original phase. Both of

TABLE I. List of the observed and calculated interplanar spacings d and intensities I of the $B3$ structure near 11 GPa. The calculation of relative intensities is discussed in Ref. [8].

(hkl)	$d_{\text{obs}} (\text{\AA})$	$d_{\text{calc}} (\text{\AA})$	$I_{\text{obs}} (\%)$	$I_{\text{calc}} (\%)$
(111)	3.174	3.175	100.0	61.0
(200)	2.745	2.749	38.5	18.3
(220)	1.946	1.944	80.2	100.0
(311)	1.658	1.658	56.2	76.3
(222)	1.591	1.587	6.5	8.3
(400)	1.374	1.375	12.4	14.6
(331)	1.263	1.262	11.8	23.8
(420)	1.228	1.230	4.8	8.1
(422)	1.124	1.122	10.2	20.2
(511)	1.058	1.058	3.0	8.8

these assumptions have been found to be generally true for the behavior of III-V compounds under pressure.

The new structure is now determined by the following procedure. The atomic volume V_a at some pressure in the new phase is estimated from the EOS of the original phase and the assumed volume change from (1) above. The lattice of the new phase is the one that has the minimum cell volume that gives a good fit to the observed diffraction lines, and whose cell volume V_c is such that V_c/V_a is very nearly a small integer. For our new phase this yields a hexagonal lattice with a four atom basis. The simplest structure that is hexagonal with a four atom basis and consistent with assumption (2) above is the NiAs ($B8$) structure.

All our sample spectra in the new phase fit well to the $B8$ structure with a nearly constant c/a ratio of 1.597 ± 0.008 . Figure 1(b) shows a typical EDXD spectrum of AlAs at 18 GPa indexed to the $B8$ structure, after the phase transformation is complete. Table II

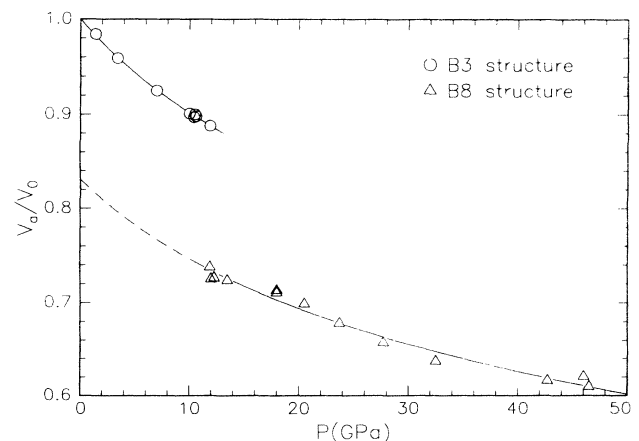


FIG. 2. Plot of reduced atomic volume, V_a/V_0 of AlAs, vs pressure, P , on uploading. V_a is the measured atomic volume and V_0 is the atomic volume of the zinc blende phase at zero pressure. Fits of the data points to the first-order Birch equation of state are shown by the curves. The values of the fitting parameters are listed in Table III.

TABLE II. List of the observed and calculated interplanar spacings d and intensities I of the $B8$ structure at 18 GPa. The lattice parameters are $a=3.600$, $c=5.740$ Å. The calculation of relative intensities is discussed in Ref. [8].

(hkl)	d_{obs} (Å)	d_{calc} (Å)	I_{obs} (%)	I_{calc} (%)
(100)	3.116	3.118	1.7	1.1
(002)	2.889	2.870	8.6	7.5
(101)	2.737	2.740	100.0	81.1
(102)	2.108	2.111	17.5	58.2
(110)	1.804	1.800	34.2	100.0
(103)	1.635	1.631	6.0	30.0
(112)	1.522	1.525	8.7	13.3
(201)	1.501	1.504	7.3	21.9
(202)	1.370	1.370	2.2	14.1

shows the observed and calculated d spacings, and integrated intensities for the nine peaks observed. The agreement of the d spacings is excellent, and the agreement of the integrated intensities is equivalent to that of the original phase before the phase transformation. Other likely candidate crystal structures for the high pressure phase were easily rejected on inspection when compared to the sample diffraction patterns. These included rock salt, β -tin, anti-NiAs, WC, and cinnabar.

The EOS of the $B8$ phase is plotted in Fig. 2. This data was also fit to the first order Birch EOS [11]. The resulting values of the three parameters are $B_0=73 \pm 7$ GPa, $B'_0=4.6 \pm 0.7$, and $V_N/V_0=0.831 \pm 0.02$. Here V_N/V_0 is the extrapolated volume of the $B8$ phase at zero pressure divided by the zero pressure volume of the original $B3$ phase. The Birch fit structural parameters for both phases are tabulated in Table III.

Three separate experiments were made from 0 to over 35 GPa. On uploading all showed the same phase transformation starting at $P_1=12$ GPa and completed by 14 GPa. Downloading data were obtained from only one of the experiments. On downloading there was none of the original $B3$ phase at 4.5 GPa. However, after the next download step to $P_1=2.0$ GPa, the sample had transformed back to the original $B3$ phase. Because of this large hysteresis all that may be inferred about the equilibrium transformation pressure P_e between the $B3$ and $B8$ phases is that it is between P_1 and P_1 . Thus $P_e=7 \pm 5$ GPa. Based on the experimental EOS's the volume change at 7 GPa is $17 \pm 1\%$.

Various theoretical calculations have been made of B_0 of the zinc blende phase of AlAs. Values (in GPa) of 86 [13], 74.1 [2], 71.0 [14], 75 ± 1 [15], and most recently 71 [16], have been reported and are consistent with our measured value of 74 ± 4 . The calculations were based on the local-density approximation pseudopotential method. The best other experimental value, 78.1, to compare to is based on extrapolated elastic constants from related compounds [17].

There is limited theoretical information available for the $B8$ phase of AlAs. In the calculations of Froyen and

TABLE III. Parameters obtained by fits of the Birch first-order equation of state to atomic volume vs uploading pressure data. V_N/V_0 is the extrapolated zero pressure atomic volume divided by the zero pressure atomic volume of the zinc blende phase.

Phase	V_N/V_0	B_0 (GPa)	B'_0
$B3$	1	74 ± 4	5.0 ± 1
$B8$	0.831	73 ± 7	4.6 ± 0.7

Cohen (FC) [2] the rock salt (rs) and NiAs structures had very nearly identical total energy vs volume curves (within the resolution of their calculations), with NiAs having the slightly lower energy. Their value of $P_e=7.6$ GPa for the zinc blende (zb) to rs transition (no other values are given for the NiAs structure) makes a reasonable comparison to our experimental value of 7 ± 5 GPa. FC's calculated value of c/a for the NiAs phase is stated to be a few percent above the ideal value of 1.633 while our measured value is 1.60. FC's value of $\Delta V/V_0$ for zb to rs structures at their P_t was 0.22 vs our value of 0.17 ± 0.01 for zb to NiAs at P_t . In a later paper Zhang and Cohen give $\Delta V/V_0=0.207$ at $P_t=7.6$ GPa for the zb to rs transition [14]. Martin has calculated $P_t=9.0$ GPa for zb to rs, and also notes that the NiAs structure had a slightly lower energy than rs [3].

It is instructive to compare the cases of AlAs to GaAs. Both compounds have almost identical lattice constants and bulk modulus at zero pressure. Both have considerable hysteresis between P_1 and P_1 for their first high pressure phase transition. But there are also some striking differences: AlAs has $P_e=7$ GPa and transforms from zinc blende to NiAs, whereas GaAs has $P_e=12$ GPa [18] and transforms from zinc blende to GaAs(II) [19], a sixfold coordinated orthorhombic structure. GaAs eventually transforms to a simple hexagonal structure at ~ 70 GPa [19]. It would be interesting to do additional high pressure experiments on AlAs to determine if it too goes to a simple hexagonal structure.

FC also give a discussion of the NiAs structure and its close relation to the rock salt structure. They point out that each cation (Al) has the same local environment as in rock salt (sixfold coordination). They interpret their slightly larger than ideal value calculated for c/a as indicating an instability towards a close packed structure.

It is also well known that for ideal c/a the anions of the NiAs structure form an hcp structure with the cations at all the octahedral sites. The cations, at the center of the octahedral holes, form a simple hexagonal array. An alternative view of this structure is each anion has six neighbors at the corners of a right trigonal prism, but each cation has eight close neighbors, six anions, and two additional cations at $\pm \frac{1}{2}c$ [20]. We may then interpret our slightly smaller than ideal measured value of c/a as indicating a tendency towards an interstitial compound. An example of such a structure is WC, which has a sim-

ple hexagonal lattice. There are many examples of elements and $A^N B^{8-N}$ compounds with high pressure structures based on the simple hexagonal lattice. These include Ge [21], Si [22,23], GaAs [19], GaSb [24], and InSb [25].

We thank the CHES staff for their technical assistance and acknowledge support by the Department of Energy under Grant No. DE-FG02-87ER-45320. We also acknowledge support by the Cornell Materials Science Center under Grant No. DMR9121654 for the use of their central facilities. We also thank Kouros Ghandehari for help with the experimental measurements and Dieter Ast for helpful discussions.

-
- [1] K. N. Tu, J. W. Mayer, and L. C. Feldman, *Electronic Thin Film Science for Electrical Engineers and Materials Scientists* (Macmillan, New York, 1992), Chaps. 7 and 8.
 - [2] S. Froyen and M. L. Cohen, *Phys. Rev. B* **28**, 3258 (1983).
 - [3] R. M. Martin, in *Proceedings of the Eighteenth International Conference on the Physics of Semiconductors, Stockholm, Sweden, 1986*, edited by O. Engström (World Scientific, Singapore, 1987), p. 639.
 - [4] B. A. Weinstein, S. K. Hark, R. D. Burnham, and R. M. Martin, *Phys. Rev. Lett.* **58**, 781 (1987).
 - [5] Q. Xia, H. Xia, and A. L. Ruoff, *J. Appl. Phys.* **73**, 8198 (1983).
 - [6] J. C. Jamieson, *Science* **139**, 845 (1963).
 - [7] *Semiconductors: Physics of Group IV Elements and III-V Compounds*, edited by K. H. Hellwege, Landolt-Börnstein, New Series, Group III, Vol. 17, Pt. a (Springer-Verlag, Berlin, 1982).
 - [8] M. Baublitz, Jr., V. Arnold, and A. L. Ruoff, *Rev. Sci. Instrum.* **52**, 1616 (1981).
 - [9] K. E. Brister, Y. K. Vohra, and A. L. Ruoff, *Rev. Sci. Instrum.* **57**, 2560 (1986).
 - [10] J. C. Jamieson, J. Fritz, and M. H. Manghnani, *Adv. Earth Planet. Sci.* **12**, 27 (1980).
 - [11] F. Birch, *J. Geophys. Res.* **83**, 1257 (1978).
 - [12] F. D. Murnaghan, *Proc. Natl. Acad. Sci. U.S.A.* **30**, 244 (1944); O. L. Anderson, *J. Phys. Chem. Solids* **27**, 547 (1966).
 - [13] J. Ihm and J. D. Joannopoulos, *Phys. Rev. B* **24**, 4191 (1981).
 - [14] S. B. Zhang and M. L. Cohen, *Phys. Rev. B* **35**, 7604 (1987).
 - [15] N. Chetty, A. Muñoz, and R. M. Martin, *Phys. Rev. B* **40**, 11934 (1989).
 - [16] P. E. Van Camp (private communication).
 - [17] S. Adachi, *J. Appl. Phys.* **58**, R1 (1985).
 - [18] J. M. Besson, J. P. Itié, A. Polian, G. Weill, J. L. Mansot, and J. Gonzalez, *Phys. Rev. B* **44**, 4214 (1991).
 - [19] S. T. Weir, Y. K. Vohra, C. A. Vanderborgh, and A. L. Ruoff, *Phys. Rev. B* **39**, 1280 (1989).
 - [20] R. G. W. Wyckoff, *Crystal Structures* (Interscience, New York, 1971), Vol. 1, pp. 123.
 - [21] Y. K. Vohra, K. E. Brister, S. Desgreniers, A. L. Ruoff, K. J. Chang, and M. L. Cohen, *Phys. Rev. Lett.* **56**, 1944 (1986).
 - [22] J. Z. Hu and I. L. Spain, *Solid State Commun.* **51**, 263 (1984).
 - [23] H. Olijnyk, S. K. Sikka, and W. B. Holzapfel, *Phys. Lett.* **103A**, 137 (1984).
 - [24] S. T. Weir, Y. K. Vohra, and A. L. Ruoff, *Phys. Rev. B* **36**, 4543 (1987).
 - [25] C. A. Vanderborgh, Y. K. Vohra, and A. L. Ruoff, *Phys. Rev. B* **40**, 12450 (1989).